

Physico-durability aspects of partial substitution via pelletized fly ash lightweight nano-silica concrete

Waleed A. Abbas, Mohammed L. Abbas

Online Publication Date: 20 Jan 2023

URL: <http://www.jresm.org/archive/resm2022.567st1025.html>

DOI: <http://dx.doi.org/10.17515/resm2022.567st1025>

Journal Abbreviation: *Res. Eng. Struct. Mater.*

To cite this article

Abbas WA, Abbas ML. Physico-durability aspects of partial substitution via pelletized fly ash lightweight nano-silica concrete. *Res. Eng. Struct. Mater.*, 2023; 9(2): 475-491.

Disclaimer

All the opinions and statements expressed in the papers are on the responsibility of author(s) and are not to be regarded as those of the journal of Research on Engineering Structures and Materials (RESM) organization or related parties. The publishers make no warranty, explicit or implied, or make any representation with respect to the contents of any article will be complete or accurate or up to date. The accuracy of any instructions, equations, or other information should be independently verified. The publisher and related parties shall not be liable for any loss, actions, claims, proceedings, demand or costs or damages whatsoever or howsoever caused arising directly or indirectly in connection with use of the information given in the journal or related means.



Published articles are freely available to users under the terms of Creative Commons Attribution - NonCommercial 4.0 International Public License, as currently displayed at [here](http://creativecommons.org/licenses/by-nc/4.0/) (the "CC BY - NC").



Research Article

Physico-durability aspects of partial substitution via pelletized fly ash lightweight nano-silica concrete

Waleed A. Abbas^a, Mohammed L. Abbas^b

Civil Engineering Dept., University of Technology- Iraq, Al-Sinaa Street, 10066 Baghdad, Iraq

Article Info

Article history:

Received 25 Oct 2022

Revised 07 Jan 2023

Accepted 19 Jan 2023

Keywords:

*High-performance
lightweight concrete;
Nano-SiO₂;
Cold-bonded;
Rapid chloride
permeability test;
Water permeability;
Drying shrinkage*

Abstract

This study's main goal is to examine the durability and shrinkage properties of high-performance lightweight concrete (HPLC) which uses lightweight synthetic fly ash instead of some natural coarse aggregate. By combining 90% fly ash and 10% Portland cement by weight in a tilted rotating pan at room temperature and curing the aggregate for 28 days, the synthetic aggregate was created using the cold bonded pelletization procedure. Then, ten combination samples were made using HPLCs by substituting natural coarse aggregate for fly ash aggregate at percentages of 0, 10, 20, 30, and 40% of the aggregate's total volume with a water binder (w/b) ratio of 0.35 both with and without the addition of nano-SiO₂ (nS). Durability characteristics, rapid chloride penetration and water permeability, were tested for 28 and 90 days, while drying shrinkage and weight loss were examined for 61 days. Results demonstrated a lower performance with control mix in terms of durability and shrinkage characteristics with increasing the coarse aggregate replacement (%) of lightweight aggregate (LWA). Additionally, nS improved the transport qualities by reducing the porosity traits and detrimental effects of synthetic LWAs. On the other hand, nS particle-related permeability decreases up to 23.34% due to a larger surface area and smaller particle size that made a permeability channel more meandering or partially closed. HPLCs mixes greatly reduce the overall shrinkage strain when adding 3% nS to HPLC specimens by 11.73% over 61 days. The statistical models that were derived indicated that the independent variables have a statistically significant impact.

© 2023 MIM Research Group. All rights reserved.

1. Introduction

Due to the lack of landfills and the vast amounts of solid waste materials, controlling solid waste management is one of the most difficult problems in our nation and around the world. Reusing and recycling demolition waste is crucial as a result of lessening this issue and looking for an environmentally friendly answer. For instance, enormous amounts of pulverized fly ash are produced by coal-fired thermal plants, yet lesser amounts can be used in the building sector. Due to the severe lack of natural aggregates, synthetic aggregate utilization in the building industry has received significant attention. Thus, the manufacturing of synthetic aggregates addresses two issues: decreasing environmental harm and averting the loss of natural resources, paving the way for sustainable growth. Cold bonding and sintering are efficient ways to manufacture lightweight aggregates. Low strength synthetic aggregates are produced via cold bonding, which requires little energy and relies on the pozzolanic reaction of fly ash to assemble tiny particles into pellet. Pelletization, a procedure that involves mixing fly ash with the right quantity of water and a binder like cement in a pelletizer, can be used to create artificial lightweight fly ash aggregates that are then further hardened using the cold bonding technique [1 – 6]. Thomas, J. and Harilal, B. [7] provide a framework for assessing the sustainability of cold-

^aCorresponding author: waleed.a.abbas@uotechnology.edu.iq

^aorcid.org/0000-0001-8287-2782, ^borcid.org/0000-0002-2284-7056

DOI: <http://dx.doi.org/10.17515/resm2022.567st1025>

Res. Eng. Struct. Mat. Vol. 9 Iss. 2 (2023) 475-491

bonded aggregates. Social, environmental, and economic aspects served as the primary evaluation criterion. These three sustainability pillars. Utilized were cold-bonded aggregates made from waste products like fly ash and quarry dust. According to this finding, cold-bonded aggregates are viable and should be taken into account when producing used concrete. The volume of binder and the distance to the raw material source were both mentioned as important considerations.

Civil infrastructures are commonly vulnerable to severe loading conditions and harsh environments, especially for structures in aggressive environments. Therefore, durability is an important feature of concrete since it strongly affects structures' maintenance costs and service life. Concrete service life is mainly influenced by permeability associated with harmful agents like chloride, water permeability, carbon dioxide (CO₂), etc. Permeability is one of the fundamental characteristics of concrete structures, as it is closely associated with durability. Concrete durability depends strongly on the ability of concrete to prevent the entry of aggressive chemical species. For this reason, the permeability of concrete is a key indicator and major index for this ability [8 - 9].

The interfacial transition zone (ITZ) between coarse aggregate and cement paste is well established to have an effect on the durability of concrete. In general, when light weight aggregate (LWA) is used, the ITZ is better than when normal weight aggregate (NWA) used [10]. In general, LWAs have more porosity than NWAs. The permeability of LWC might not always be greater than that of NWC. Increasing porosity, enhancing the transition zone between the surface, enhancing cement hydration owing to internal curing, and limiting micro cracking that may affect chloride ions and water transport in the concrete are just a few of the ways that LWCs differ from NWCs. Since linking the pore system has been crucial, the transport properties of LWC in comparison to NWC rely on which of these variables is prominent. The quality of the LWC matrix is typically more significant in regulating the concrete's transport properties [11-12].

The growth of high strength-performance concrete for specific applications results from the retro-gradation of concrete structures in aggressive environments due to its better engineering and performance properties, mainly common characteristics of good workability, high strength, low porosity, and fine pore structure. These, in turn, enhance the concrete resistance to the penetration of harmful substances like chloride ions, carbon dioxide (CO₂), oxygen, and water permeability [13].

In recent years, the incorporation of cementitious materials such as fly ash, silica fume, and ground granulated blast furnace slag (GGBFS) into concrete has been shown to increase the resistance to the deterioration of aggressive media and permeations while lowering the cost of concrete production, preserving resources and energy, and reducing the impact of environmental pollution [14]. The addition of nano-silica has generally improved the concrete performance due to experimental results [15-16] according to its pozzolanic reaction and filler effect. [17] Reported the pozzolanic reaction and the rate of cement hydration increased when the addition of nS because of the nS small particle size, which provides a larger surface area. In their discussion of the impact of 3.8% colloidal nS on the durability characteristics of self-compacting concrete (SCC), Quercia et al. [18] discovered that the pore was less linked and finer. Mohseni E. and Ranjbar M. [13] presented the durability properties of high-performance concrete incorporation nano TiO₂ and fly ash. They concluded the concrete containing nano-TiO₂ significantly improved durability performance in capillary water absorption and chloride diffusion and resistance to sulphuric acid attack by including the replacement of cement of 1% nanoparticles and 30% FA combination. [19] has been claimed that the inclusion of nano-SiO₂ and TiO₂ can refine pore structures, reducing the permeability of concrete to chloride. For up to 56 days, Kayyali O. and Haque M. [20] looked at the drying shrinkage of LWC with coarse and fine sintered

fly ash aggregate. In terms of dry density and compressive strength, the concrete had values of 1900 kg/m³ and 70 MPa, respectively. They came to the conclusion that LWC shrank less while drying than NWC. In a 57-day study, Gesoğlu et al. [21] investigated the drying, restricted, and autogenous shrinkage of high strength concrete containing synthetic fly ash and blast furnace slag aggregates. Cold bonding was used to create the substitute aggregates. The test findings showed that high-strength concrete with 20% synthetic slag aggregate had better mechanical properties. Additionally, slag aggregate added to high strength concrete prolonged the cracking period and resulted in a finer crack with decreased free shrinkage. All high strength concretes, including those with synthetic aggregates, also showed a discernible decline. Atmaca et al. [22] looked into how 3% nS particles affected HSLWCs' compressive strength, sorptivity, splitting tensile strength, and gas permeability. They came to the conclusion that, in 28 and 90 days, nS particles in HSLWCs provide better compressive strength and splitting tensile strength. The included nS samples showed a decrease in gas permeability and water sorptivity.

The results of an investigation by Kasm M. et al. [23] studied the effect of the micro-steel fiber, pelletized fly ash lightweight aggregate, and microsilica content on the mechanical properties of high-performance cementitious composite (HPCC) and shrinkage behavior showed that the steel fiber volume fraction had a positive effect. Microsilica also has the ability to neutralize the drawbacks of synthetic lightweight aggregate. Kseniia U. [24] demonstrated in his research for a C25/30 concrete with cold-bonded fly ash aggregate, that the linear expansion coefficient is $14.8 \times 10^{-6} \text{ K}^{-1}$, the modulus of elasticity is $18 \times 10^9 \text{ Pa}$, the compressive strength after 28 days is 37.8 MPa, and the flexural strength is 4.9 MPa. The kinetics of heat emission and cement hydration were unaffected by water presoaking lightweight aggregates, while air shrinkage deformation was positively affected.

By using the cold-bonded approach, Jiayi L. et al. [25] created a novel type of artificial lightweight aggregates from a type of municipal woody biomass waste ash (MWBA). Municipal woody biomass waste ash aggregate (MWBA) performance was examined in relation to the effects of varying cement content 5, 10, 15, and 20%, curing time 3, 7, 14, and 28 days, and rotation speed 30, 40, 50, and 60 rpm on particle size fractions of fraction 4 mm–10 mm, 10 mm–16 mm, 16 mm–20 mm. The water content 20-33%, rotation speed 30, 40, 50, and 60 rpm, and rotation angle 30–60°. The bulk density of the MWBA ranges from 841 to 1058 kg/m³. Additionally, it was shown that 27–29% water concentration is ideal for MWBA manufacture. The rotation speed and angle that produced the maximum granulation efficiency were 55° and 60 rpm. The MWBA with 20% cement content had the maximum compressive strength after 28 days of curing was 2.6 MPa. In order to successfully recycle MWBA and maybe granulate MWBA into lightweight aggregate that can be used in concrete, the study offers an alternate option. The work suggests a different way to efficiently recycle MWBA and perhaps even granulate it into lightweight material that can be used in concrete.

Therefore, the primary objective of this work is to investigate the shrinkage and durability properties of nano high performance lightweight concrete. In order to create HPLCs, fly ash was cold-bonded pelletized to create the alternative LWA. LWAs from 0 to 40% by 10% increments were used to partially replace the typical coarse aggregate. Thus, ten distinct HPLC mixes with and without nS were created, each with a 420 kg/m³ binder content and a 0.35 w/b ratio. The water permeability, capillary water absorption, chloride ion permeability, drying shrinkage, and weight loss of the created concrete mixtures were all examined to determine their durability.

2. Experimental Study

2.1. Materials

This experiment made use of Portland cement (PC) type I complies with [BS. EN197-1], fly ash (FA) meets the requirements of ASTM C618 [26], nano-SiO₂ (nS), and high range water reducing admixture (HRWRA) had a specific gravity of 1.07 and was used as a superplasticizer (SP). The physical characteristics and chemical compositions of the materials used are stipulated in Table 1.

Table 1. Chemical compositions and physical characteristics of materials used

	PC	FA	nS
Physical Characteristics			
Fineness (Blain) (cm ² /g)	3950	3800	-
Specific Gravity (s.g.)	3.16	2.06	2.3
Specific surface area (BET) (m ² /g)	-	-	150 ± 15
Average primary particle size (nm)	-	-	14
Chemical composition (%)			
Silicon Dioxide, SiO ₂	19.7	57.2	99.8
Calcium Oxide, CaO	62.13	2.24	-
Ferric Oxide, Fe ₂ O ₃	2.9	7.1	-
Aluminum Oxide, Al ₂ O ₃	5.15	24.4	-
Sulfur Trioxide, SO ₃	2.65	0.29	-
Magnesium Oxide, MgO	1.2	2.4	-
Sodium Oxide, Na ₂ O	0.17	0.38	-
Potassium Oxide, K ₂ O	0.89	3.37	-
Loss on Ignition	2.99	1.52	≤ 1.0

2.2. Synthetic Aggregates

The fabrication of the synthetic LWAs in the pelletized machine at room temperature began the experimental program with the cold bonding of FA and PC. As shown in (Fig. 1), a pelletizer machine for this has an 80 cm diameter and a 35 cm depth. The horizontal angle of the pelletizer disc was 45 degrees, and its rotational speed was 42 rpm. The dry powder, which was poured out into the pelletizing pan and allowed to mix until a well-blended-mixture was reached to create the synthetic LWA, was composed of 90% FA class (F) and 10% PC by weight. The pressurized water injection mechanism controlled the amount of water sprayed to be about 20% by weight of the dry mixed mixture. In this procedure, the coagulant was water. After 10 minutes of the first stage's length, the spheroidal fly ash pellets were obtained. A further 10 minutes of agglomeration time is required for appropriate stiffness and compressed fresh pellets. After the pelletization process is complete, the fresh pellets must be saved in sealed plastic bags for a 28-day self-curing period in the curing room to harden at a temperature and relative humidity of 22°C and 70%, respectively. Ultimately, the solidified LWAs were sieved as lightweight coarse aggregate (4-16 mm) to replace the coarse natural utilized to create HPLCs. According to ASTM C 127[27], specific gravity and 24-hour water absorption for LWAs were approximately 1.64g/cm³ and 21.12%, respectively. The fine and coarse materials used

were sand and gravel, which naturally have specific gravities of 2.7 and 2.67, respectively. Table 2 displays the sieve analysis grade for natural and LWA.

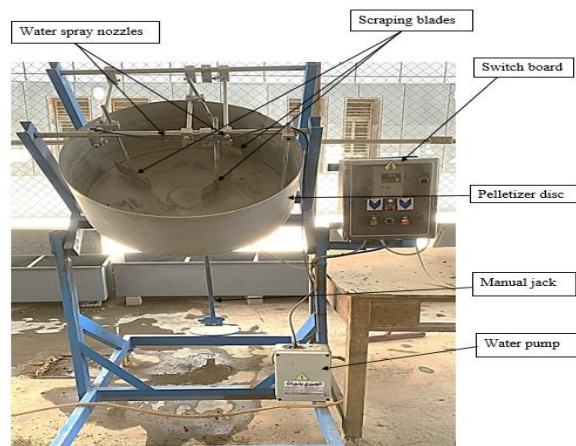


Fig. 1 Pelletizer machine

Table 2. Physical characteristics and sieve analysis of aggregates

Sieve size (mm)	Natural Aggregate		Lightweight Aggregate (%)
	Sand	Gravel	4-16 mm
16	100	100	100
8	100	31	81
4	95	0.3	0
2	59	0	0
1	37.8	0	0
0.5	24	0	0
0.25	6	0	0
Fineness modulus (%)	2.79	5.68	5.15
Specific gravity	2.70	2.67	1.64

2.3. Mixes Proportion Details

The second part of the investigation program, which involved the creation of ten HPLC mixes total and showed how LWAs can partially replace natural coarse aggregate at different volume fractions ranging from 0% to 40% in increments of 10%, revealed the durability and shrinkage properties of concrete mixes. The next step was to plan two series: the first involved replacing synthetic coarse lightweight aggregate with coarse natural aggregate free of nanoparticles, and the second involved replacing LWAs with natural coarse aggregate that had nanoparticles. To provide the necessary workability, various concentrations of HRWRA were utilized. To create HPLC mixtures, a 30 L capacity power-driven rotating pan apparatus was employed. The control mix contained only natural aggregate. The goal of all the mixes was to get a $150\text{ mm} \pm 20\text{ mm}$ slump. To achieve consistent workability, different concentrations of HRWRA (SP) have been utilized in each mixture.

Table 3. Mix proportions details for HPLCs

Mix series	Mix designation	w/b	binder	PC	FA	nS	water	SP	sand	Gravel	LWA
Series I	nS0%, LWA0%	0.35	420	336.0	84	0.0	147.0	6.3	942.5	932.0	0.0
	nS0%, LWA10%	0.35	420	336.0	84	0.0	147.0	6.3	942.5	838.8	57.2
	nS0%, LWA20%	0.35	420	336.0	84	0.0	147.0	6.3	942.5	745.6	114.5
	nS0%, LWA30%	0.35	420	336.0	84	0.0	147.0	6.3	942.5	652.4	171.7
	nS0%, LWA40%	0.35	420	336.0	84	0.0	147.0	6.3	942.5	559.2	229.0
Series II	nS3%, LWA0%	0.35	420	323.4	84	12.6	147.0	9.2	936.4	926.0	0.0
	nS3%, LWA10%	0.35	420	323.4	84	12.6	147.0	9.2	936.4	833.4	56.9
	nS3%, LWA20%	0.35	420	323.4	84	12.6	147.0	9.2	936.4	740.8	113.8
	nS3%, LWA30%	0.35	420	323.4	84	12.6	147.0	9.2	936.4	648.2	170.6
	nS3%, LWA40%	0.35	420	323.4	84	12.6	147.0	9.2	936.4	555.6	227.5

* All weights are in **kg/m³** units.

2.4. Test Methods

Regarding BS EN (12390-8)[28], the water penetration depth of HPC containing LWA for 28 and 90 days was adapted. For this, 150 mm cube specimens were pressurized with water at a pressure of $500 \pm 50 \text{ kPa}$ for 72 hours. The middle section of the specimens was divided, and the greatest pressurized water penetration was gauged in millimeters. The average outcomes of three samples of the mix were considered for each testing interval. If the water penetration does not rise by 30 mm after concrete comes into contact with aggressive media, chemical attacks might be regarded to be resistant. ASTM C1202[29] was used to analyze the rapid chloride permeability test (RCPT) for HPLC. As stated in[29], the middle portion of each cylinder specimen measuring approximately $100 \times 200 \text{ mm}$ was cut into three-disc samples measuring 50 mm in height and 100 mm in diameter. At 28 and 90 days, the test was conducted. The disk samples were then placed on a test cell with one side of the specimens in contact with 0.3M sodium hydroxide and the other in contact with a 3% solution of sodium chloride. A direct voltage of $60 \pm 01V$ was applied between the faces. Every 30 minutes, data on the concrete's resistance to chloride ion permeability were archived in order to track the charge that moved through

the samples over the course of six hours. The total charge in $A.s$ ($amperes \times seconds = coulombs$) that passed through the specimens was determined using Simpson's integration and present and time historical knowledge[28]. The drying shrinkage of HPLCs was calculated through three $70 \times 70 \times 280$ mm prisms due to ASTM C157[30]. The gage length was settled on the top surface of each specimen by the mean of the glued pin as soon as demolding the prisms. An electronic dial gauge extensometer was used to measure the change length over 200 mm, accurate to 0.002 strains. For the first 21 days, measurements were taken every day; thereafter, they were taken three times per week. Investigations into weight loss were conducted using the same prism. Weight loss and strain variations due to drying shrinkage were recorded over a 61-day period at a drying temperature of 23.2 °C and a relative humidity of 50.5%.

3. Results and Discussions

3.1. Water Permeability

The test uses a range of pressures to calculate the depth of water penetration into the concrete. (Fig. 2) displays the variation in the water penetration depth of HPLCs at 28 and 90 days. As anticipated, the HPC incorporating LWA had water penetration rates at 90 days that are less than 28 days. Additionally, adding LWA to HPC resulted in the construction of more water-absorbent concretes, and the effect grew stronger when LWA content was increased. It is obvious from (Fig. 2) that the water penetration depth goes an upward trend with partial replacement of natural aggregate by LWA. When adding 3% nS with the same replacement amount of LWA, there is a tendency for decline. The lowest value of water penetration depth was measured for nS3%, LWA 0% as 11.5 and 7.5mm, in contrast to the largest penetration depth, which was recorded for nS0 %, LWA40% as 27mm and 21mm at 28 and 90 days, respectively. The porous nature of LWAs accounts for the high penetration depth. Under pressure, water can easily pass-through aggregates, resulting in deeper water penetration in the HPC than that of the mix nS0%, LWA0%, which contains LWAs.

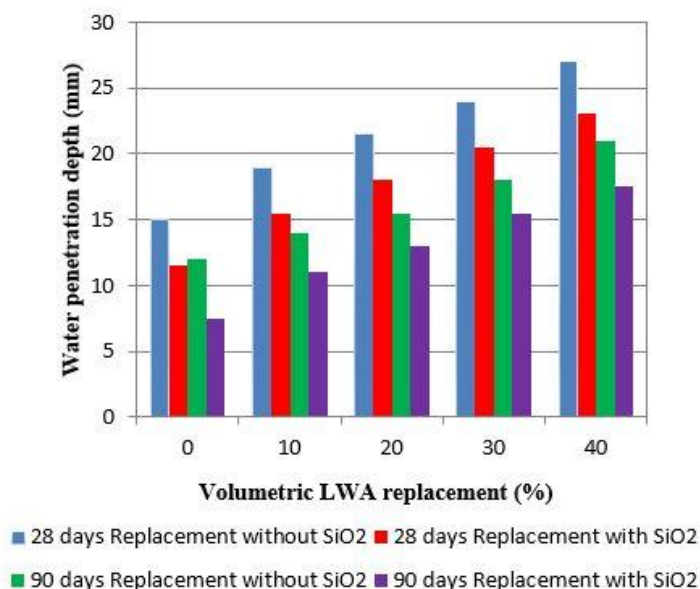


Fig. 2 The 28- and 90-days water penetration values of HPLCs.

This reply supports the findings of some researchers who claimed that numerous synthesized LWAs in concrete increased water penetration [31]. However, when 3% nS particles are added with the same level of LWA substitution, there is a noticeable drop of roughly 14.5-23.3 %. Since the pore structure of HPC substantially affects its endurance, it can be said that adding nS as a mineral admixture has a good impact on the mechanism. However, by filling the voids during the development of the cement paste using aggregate, the ITZ might be impacted [32]. HPLC notices a systematic reduction in water permeability after the addition of concrete with 3% nS particles. The water permeability reached 37.5% when 3% nS was added. The findings of several investigations [33-34] are supported by these findings. In general, high depth water permeability is a sign of low concrete material durability [35]. It is clear that using nS particles as cementitious material significantly lowers the water permeability of HPLC while maintaining the same level of LWA replacement.

3.2. Rapid Chloride Penetration

The infiltration of water containing chloride and other hostile ions into the concrete is the main factor influencing the physical and chemical deterioration process. This procedure, which primarily regulates the microstructure of concrete is connected to water infiltration and ion transport [36]. The total charged A.s (coulombs) passed through concrete disc specimens during 6 hours as a function of electro-migration, which was determined by ASTM C 1202[29] which confirmed concrete's resistance to chloride ion penetration.

(Fig. 3) displays graphically the total charge that was passed through HPLCs throughout the course of 28 and 90 days.

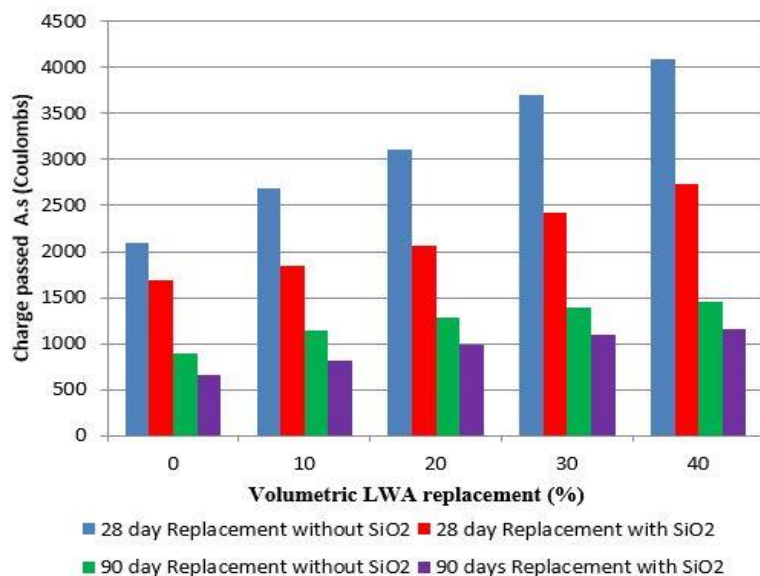


Fig. 3 The 28 and 90-day RCPT values of HPLCs

As the LWAs were replaced with natural aggregate, the results demonstrate a steady rise in chloride-ion permeability. With an increase in the replacement amount, this effect becomes much more noticeable. High chloride permeability refers to the maximum charge that has been observed passing through HPCs, including LWAs, at a coarse aggregate replacement of 40% of 4089 A.s (coulombs) at 28 days without nS. According to ASTM

C1202[29], the total charge transmitted through HPLCs in contrast to LWAs without nS particles in the range between 2000-4000A.s resulted in a moderate categorization of chloride penetration. The pozzolanic reaction and effects of the filler nS particles, which make the ion pathway more difficult or partially blocked are evident from (Fig. 3) that the HPLCs showed a notable diminish to the second series after the addition of 3% nS particles, with the same replacement of LWAs[37]. For 28 days, the 2nd series charges passed were measured as 1690.6A.s, 1847.3A.s, 2067.8 A.s, 2429.1A.s, and 2740A.s for replacements 0-40% of LWAs with nS particles, and the decrease percentages were 19.52%, 31.32%, 33.30%, 34.34%, and 32.99% respectively. Moreover, zero and ten replacement percentages were classified as low chloride permeability, while 20%, 30%, and 40% were classified as moderate chloride permeability concerning ASTM C 1202[29]. These classes were shown to have low chloride permeability with 30 and 40% at 90 days, despite having been seen as very low in terms of 0%, 10%, and 20% coarse aggregate replacement with nS particles. The chloride permeability values are also significantly impacted by the extended testing period of 28 to 90 days.

3.3. Drying Shrinkage and Weight Loss

Long-term drying shrinkage depends on curing temperature, degree of hydration, w/c, relative humidity, aggregate type and characteristics, drying period, admixtures, and cement composition. (Fig. 4) and (Fig. 5) show the changes in total shrinkage for HPC with LWA at a 61-day drying time.

Overall, it is evident that as drying progresses for all mixes gradually reduces the total shrinkage rate of HPC including LWA. On the other hand, (Fig. 4) demonstrates how the drying shrinkage rate rose as LWA largely replaced the natural aggregate. The majority of the entire shrinkage's growth nearly occurred in the first three weeks. The lowest shrinkage strain of $448 \mu\epsilon$ for series I in (Fig. 4) was recorded at 61 days for nS% and LWA0%, while HPC contained 40% LWA was recorded the largest shrinkage value $597 \mu\epsilon$. The total shrinkage strain of HPCs was reduced by 6.47, 16.07, 24.77, and 33.26 %, respectively, for mixtures of nS0% and LWA10%, nS0% and LWA20%, nS0% and LWA30%, nS0% and LWA40%, when compared to the control mix of nS0% and LWA0%. The usage of LWA in the mixtures may be referred to as the cause of the increase in the overall shrinkage strain of HPCs in this study. Additionally, the high porosity of LWA and its reduced stiffness as a result of its rapid absorption rate contribute to concrete's increased drying shrinkage. These results were reported by other previous researchers [21, 38-39].

From (Fig. 5) for series II, it is evident the influence of replacing cement with nS was to fade the strain development of the drying shrinkage. The addition of 3%nS to the HPLC mixes resulted in a notable improvement in the drying shrinkage by 9.37%, 9.01%, 11.73%, 10.37%, and 9.88% after 61 days, respectively. This improvement was seen in comparison to the two series, as shown in (Fig. 5) the results were confirmed the findings in the study conducted by [40-41]. An extreme fall development at an early age test in the values of drying shrinkage of HPLCs according to (Fig. 5) although the strain development of HPLCs was affected by nS incorporation, LWA coarse aggregate replacement and aggregate type have the main role especially at the initial reading. Moreover, nS efficiency displayed a positive effect and seemed to be more pronounced on the higher coarse aggregate replacement of LWA than at the lowest replacement in strain development. For instance, the drying shrinkage for series I, 448, 477, 520, 559, and $597 \mu\epsilon$. In comparison, it is found for series II, 406, 434, 459, 502, and $538 \mu\epsilon$. (Figs. 6 & 7) depicts series I and II, respectively, the changes in weight loss over time as a result of the drying period. Similar tendencies to the drying shrinkage were revealed by HPC combined with LWA. However,

adding LWA to HPC showed a greater weight reduction, although 3% nS containing HPLWCs showed a smaller weight loss than the series I.

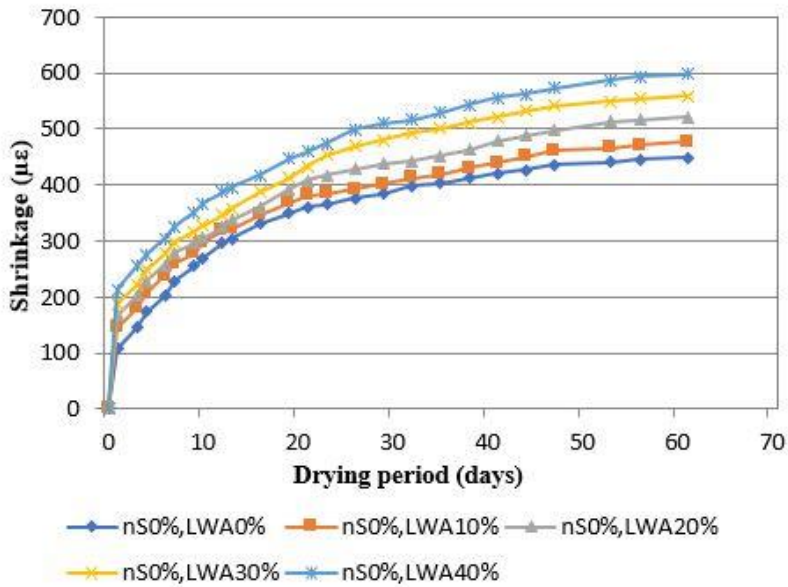


Fig. 4 Drying shrinkage for HPLCs without nS

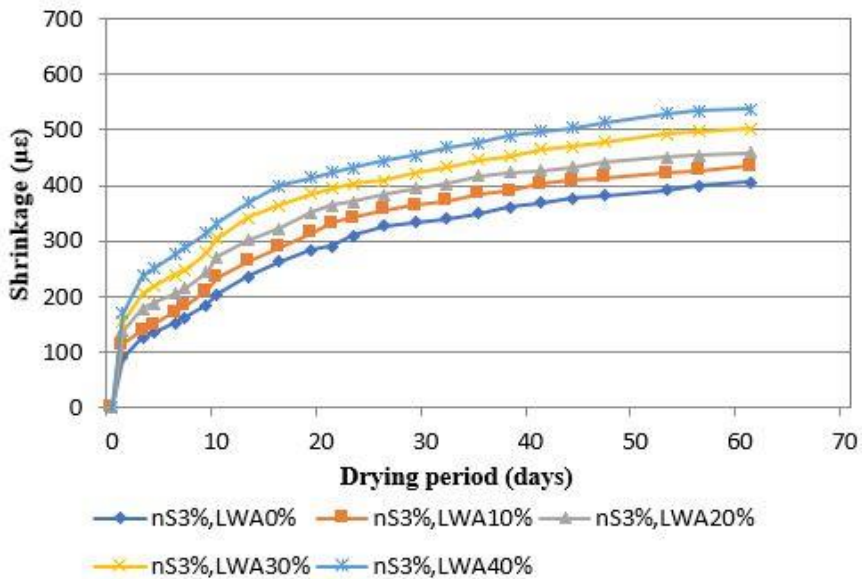


Fig. 5. Drying shrinkage for HPLCs with nS.

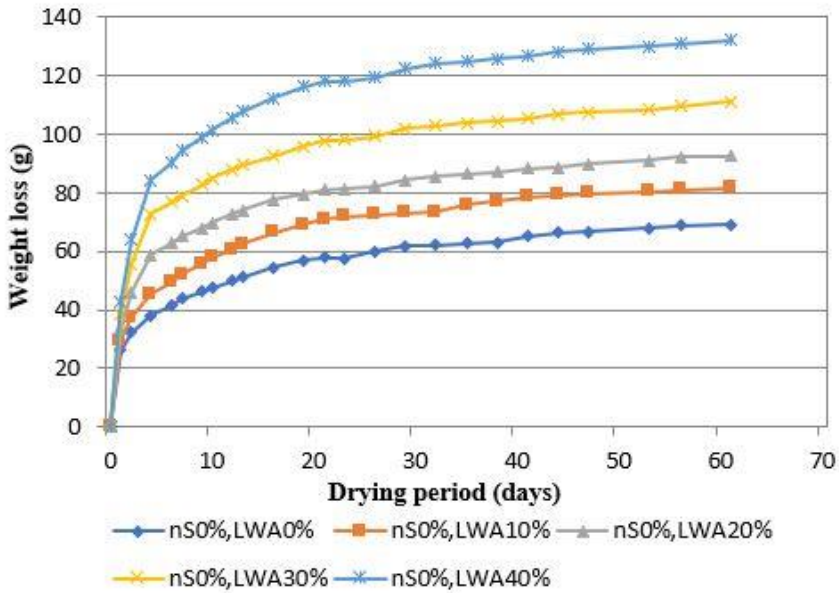


Fig. 6 Weight loss for HPLCs without nS.

After a week of drying, the difference in weight loss between the HPLC series I and II was easier to identify. It was subsequently discovered that the disparities tend to get bigger as the drying time gets longer. The percentage of weight loss increased when NWAs were switched out for LWAs, but this rise in percentage was more obvious as the coarse aggregate replacement rose.

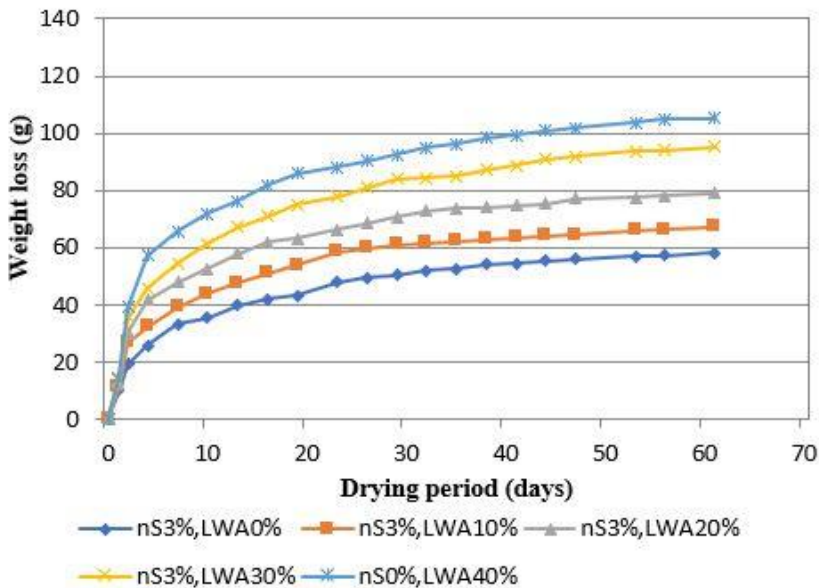


Fig. 7 Weight loss for HPLCs with nS.

For instance, the maximum weight loss for nS0% and LWA 0% in series I was 69.22 gr as opposed to 81.60, 91.57, 111.02, and 132.18 gr for nS0% and LWA 10%, nS0%, and LWA 20%, nS0%, and LWA 30%, and nS0% and LWA 40%, respectively. The incorporation of nS into HPLC combination inhibits weight loss. For instance, a maximum weight loss of series II of nS3% and LWA0%, nS3% and LWA10%, nS3% and LWA20%, nS3% and LWA30%, nS3% and LWA40% was 58.24, 67.31, 78.99, 95.18 and 105.12 gr, respectively, compared with series I with the same coarse aggregate replacement without nS. The results of weight loss measurements using HPLCs suggested that there is no direct correlation between weight loss and drying shrinkage readings. The single weight loss parameter cannot adequately explain the variations in the drying shrinkage of concrete since the shrinkage of concrete is coupled to other parameters and weight loss [42-43].

4. Statistical Analysis

The results of the analysis of variance (ANOVA) are shown in Table 4 to show whether the status of an independent variable has any impact on the dependent variables or not. The statistical evaluation of GLM-ANOVA method was performed with Minitab 17 software and a multiple linear regression method was performed with SPSS 26 software. Durability characteristics, such as water permeability and chloride penetration, were assigned as dependent variables and studied. Calculation of the experimental parameter validation was done using the general linear model analysis of variance (GLM-ANOVA), as indicated in the equations below; Eq(1) for water permeability and Eq(2) for chloride penetration. Figs. 8 & 9 show the normal P-P plot standardized residual for water permeability and rapid chloride penetration models, respectively. The independent criteria, however, were coarse aggregate replacement, Ns(%), and testing age on the 28 and 90 days.

When used in a statistical study with a 0.05 significant level, the parameter is acceptable as a significant factor smaller than that. Additionally, the percent contribution was determined to provide a general understanding of the strength of each independent parameter's influence on the dependent component. By dividing the sequential sum of squares value of an independent factor by the sum of squares of each dependent factor, the percent contributions shown in the eighth column were determined. The effectiveness of the independent component is shown by a larger percent contribution value. All independent variables have a statistically significant impact on the water permeability and chloride penetration; it may be inferred from the statistical analysis in Table 4. However, for the chloride penetration of concrete mixtures, the coarse aggregate replacement is not a statically important quantity. The most efficient independent component for the water permeability is the coarse aggregate replacement, which has a contribution value of 58.89%. The nS parameter, with values of 12.65 and 11.10%, respectively, has the least impact on the water permeability and chloride penetration. According to a statistical analysis of the RCPT results, the most important variable affecting the combinations is testing age, which has a contribution value of 66.04%. The coarse aggregate replacement has also had an impact on the RCPT model, though not to the same extent as water permeability.

$$W.P. = 18.283 - 1.133 \times Ns + 0.259 \times C.A.R. - 0.081 \times T.A. \quad (1)$$

$$R.C.P. = 3151.975 - 212.607 \times Ns + 25.753 \times C.A.R. - 25.095 \times T.A. \quad (2)$$

Where, W.P.: Water Permeability (mm.), Ns: Nano silica (%), C.A.R.: Coarse Aggregate Replacement (%), T.A.: Testing Age (days), R.C.P.: Rapid Chloride Penetration [A.s (coulombs)].

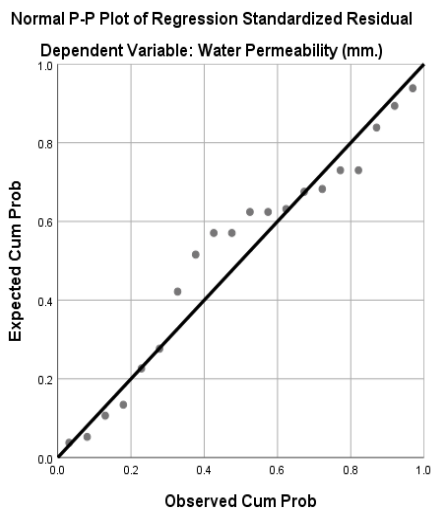


Fig. 8 Normal P-P plot standardized residual for water permeability model

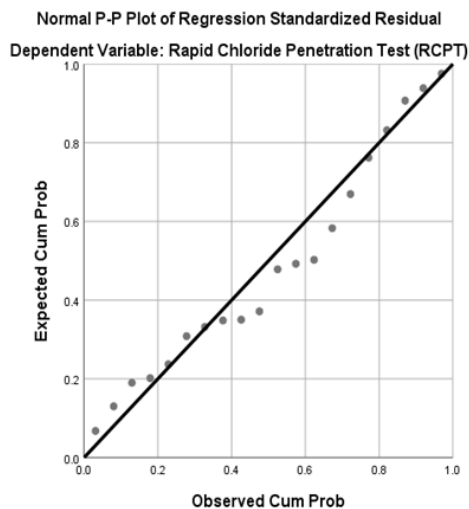


Fig. 9 Normal P-P plot standardized residual for rapid chloride penetration model

Table 4. A statistical analysis of concrete's durability characteristics.

Dependent Element	Unbiased Variable	Squares Added Sequentially	Computed F	R-Square %	P Value	Significance	Contribution %
Water Permeability	The coarse aggregate replacement (%)	269.125	172.350		0.000	Yes	58.89
	nS (%)	57.800	148.060	98.3	0.000	Yes	12.65
	Testing age (days)	125.000	320.200		0.000	Yes	27.35
	Error	5.075	-		-	-	1.11
	Total	457.000	375.872		0.000	-	-
Rapid Chloride Penetration	The coarse aggregate replacement (%)	2659772	5.66		0.000	Yes	14.50
	nS (%)	2034072	17.31	90.1	0.000	Yes	11.10
	Testing age (days)	12104124	102.98		0.000	Yes	66.04
	Error	1527957	-		-	-	8.33
	Total	18325925	58.341		0.000	-	-

5. Conclusions

The following conclusions can be reached in light of the research's findings and the materials used:

- Each HPLC combination was made to produce a slump of 150 ± 20 mm. Because nS have a tiny particle size and large surface area, the amount of HRWRA was increased from 6.3 - 9.2 % with the introduction of 3% nS to keep within the range of the required slump.
- When compared to the reference mix, a systematic rise in chloride penetration was seen as the LWAs increased due to the porous structure and high level of permeability. The pozzolanic reaction and filler effect of the nS particles, which make the ion pathway more difficult or partially blocked, caused the HPLCs with nS particles to exhibit a striking decrease in chloride permeability with the same coarse aggregate replacement of LWAs.
- As was predicted, the coarse aggregate replacement of LWAs in the mixtures led to an increase in the water penetration rates. It has been shown that the permeability decreases by up to 23.34% when nS particles are used.
- Regardless of the LWA coarse aggregate replacement, it was found that the total shrinkage strains at 61 days were higher for lightweight concrete than for normal weight concrete. This was attributed to LWA's reduced stiffness from high absorption and high porosity, which also contributed to an increase in concrete's drying shrinkage.
- The presence of 3% nS in HPLC specimens reduces drying shrinkage of 61 days by 9.37%, 9.01%, 11.73%, 10.37%, and 9.88%, respectively, while maintaining the same coarse aggregate replacement of LWA. Additionally, nS efficiency demonstrated a favorable impact on LWA coarse aggregate replacement at higher levels than at the lowest levels during strain development. Summarizing the findings, it can be said that nS can be added to LWAs to counteract their negative effects.
- The addition of nS reduced the rate of weight loss due to the drying of the concrete. Especially for mixtures having a higher rate of coarse aggregate replacement of LWA. The research showed that nS incorporation, LWA coarse aggregate replacement, aggregate type and porosity have the main role in affecting the weight loss of concrete especially at the initial readings.
- The statistical analysis of the experimental test results indicated that the most important factor influencing chloride penetration was testing age, whereas it was a coarse aggregate replacement for water permeability. Moreover, the statistical evaluation exhibited that coarse aggregate replacement had no effect on chloride penetration. But it could be realized from the statistical evaluation that the least influential parameter on water permeability and RCPT was nS particles .

References

- [1] Kayali O. Fly ash lightweight aggregates in high performance concrete. *Construction and Building Materials*. 2008;22(12):2393-9. <https://doi.org/10.1016/j.conbuildmat.2007.09.001>
- [2] Joseph G, Ramamurthy K. Influence of fly ash on strength and sorption characteristics of cold-bonded fly ash aggregate concrete. *Construction and Building Materials* [Internet]. 2009;23(5):1862-70. <https://doi.org/10.1016/j.conbuildmat.2008.09.018>
- [3] Baykal G, Döven AG. Utilization of fly ash by pelletization process; theory, application areas and research results. *Resources, Conservation and Recycling*. 2000;30(1):59-77. [https://doi.org/10.1016/S0921-3449\(00\)00042-2](https://doi.org/10.1016/S0921-3449(00)00042-2)

- [4] Zakaria M, Cabrera JG. Performance and durability of concrete made with demolition waste and artificial fly ash-clay aggregates. *Waste Management*. 1996;16(1-3):151-8. [https://doi.org/10.1016/S0956-053X\(96\)00038-4](https://doi.org/10.1016/S0956-053X(96)00038-4)
- [5] Tajra F, Elrahman MA, Stephan D. The production and properties of cold-bonded aggregate and its applications in concrete: A review. *Construction and Building Materials*. 2019;225:29-43. <https://doi.org/10.1016/j.conbuildmat.2019.07.219>
- [6] Raj KR, Vasudev R. Experimental Investigation on Artificial Light Weight Fly Ash Aggregates in Concrete. *Lecture Notes in Civil Engineering*. 2022;171:73-84. https://doi.org/10.1007/978-3-030-80312-4_7
- [7] Thomas J, Harilal B. Sustainability evaluation of cold-bonded aggregates made from waste materials. *Journal of Cleaner Production*. 2019;237. <https://doi.org/10.1016/j.jclepro.2019.117788>
- [8] Du H, Gao HJ, Pang SD. Improvement in concrete resistance against water and chloride ingress by adding graphene nanoplatelet. *Cement and Concrete Research* [Internet]. 2016;83:114-23. <https://doi.org/10.1016/j.cemconres.2016.02.005>
- [9] Valentini L, Ferrari G, Russo V, Štefančič M, Zalar Serjun V, Artioli G. Use of nanocomposites as permeability reducing admixtures. *Journal of the American Ceramic Society*. 2018;101(9):4275-84. <https://doi.org/10.1111/jace.15548>
- [10] Zhang MH, Gjörv OE. Microstructure of the interfacial zone between lightweight aggregate and cement paste. *Cement and Concrete Research*. 1990;20(4):610-8. [https://doi.org/10.1016/0008-8846\(90\)90103-5](https://doi.org/10.1016/0008-8846(90)90103-5)
- [11] Liu X, Chia KS, Zhang MH. Development of lightweight concrete with high resistance to water and chloride-ion penetration. *Cement and Concrete Composites* [Internet]. 2010;32(10):757-66. <https://doi.org/10.1016/j.cemconcomp.2010.08.005>
- [12] Chia KS, Zhang MH. Water permeability and chloride penetrability of high-strength lightweight aggregate concrete. *Cement and Concrete Research*. 2002;32(4):639-45. [https://doi.org/10.1016/S0008-8846\(01\)00738-4](https://doi.org/10.1016/S0008-8846(01)00738-4)
- [13] Mohseni E, Ranjbar MM, Tsavdaridis KD. RETRACTED: Durability properties of high-performance concrete incorporating nano-TiO₂ and fly ash. *American Journal of Engineering and Applied Sciences*. 2015;8(4):519-26. <https://doi.org/10.3844/ajeassp.2015.519.526>
- [14] Shi H sheng, Xu B wan, Zhou X chen. Influence of mineral admixtures on compressive strength, gas permeability and carbonation of high performance concrete. *Construction and Building Materials* [Internet]. 2009;23(5):1980-5. <https://doi.org/10.1016/j.conbuildmat.2008.08.021>
- [15] Raiess Ghasemi AM, Parhizkar T, Ramezani pour AA. Influence of colloidal nano-SiO₂ addition as silica fume replacement material in properties of concrete. 2nd. *International Conference on Sustainable Construction Materials and Technologies*. 2010;23-30. Universita Politecnica delle Marche, Ancona, Italy. ISBN 978-1-4507-1488-4. www.claisse.info/Proceedings.htm, 2010.
- [16] Li H, Xiao HG, Yuan J, Ou J. Microstructure of cement mortar with nano-particles. *Composites Part B: Engineering*. 2004;35(2):185-9. [https://doi.org/10.1016/S1359-8368\(03\)00052-0](https://doi.org/10.1016/S1359-8368(03)00052-0)
- [17] Belkowitz JS. AN INVESTIGATION OF NANO SILICA IN THE CEMENT HYDRATION PROCESS [Internet]. ProQuest LLC. 2009.
- [18] Quercia G, Spiesz P, Hüsken G, Brouwers HJH. SCC modification by use of amorphous nano-silica. *Cement and Concrete Composites* [Internet]. 2014;45:69-81. <https://doi.org/10.1016/j.cemconcomp.2013.09.001>
- [19] Zhang MH, Li H. Pore structure and chloride permeability of concrete containing nano-particles for pavement. *Construction and Building Materials* [Internet]. 2011;25(2):608-16. <https://doi.org/10.1016/j.conbuildmat.2010.07.032>
- [20] Kayyali OA, Haque MN. A new generation of structural lightweight concrete. *American Concrete Institute, ACI Special Publication*. 1997;SP-171:569-88.

- [21] Gesoglu M, Güneyisi E, Ismael ANI, Öz HÖ. Internal curing of high-strength concretes using artificial aggregates as water reservoirs. *ACI Materials Journal*. 2015;112(6):809-19. <https://doi.org/10.14359/51687904>
- [22] Atmaca N, Abbas ML, Atmaca A. Effects of nano-silica on the gas permeability, durability and mechanical properties of high-strength lightweight concrete. *Construction and Building Materials* [Internet]. 2017;147:17-26. <https://doi.org/10.1016/j.conbuildmat.2017.04.156>
- [23] Mermerdaş K, İpek S, Algın Z, Ekmen Ş, Güneş İ. Combined effects of microsilica, steel fibre and artificial lightweight aggregate on the shrinkage and mechanical performance of high strength cementitious composite. *Construction and Building Materials*. 2020;262. <https://doi.org/10.1016/j.conbuildmat.2020.120048>
- [24] Usanova K. Properties of Cold-Bonded Fly Ash Lightweight Aggregate Concretes. *Lecture Notes in Civil Engineering*. 2020;70:507-16.
- [25] Lin J, Mo KH, Goh Y, Onn CC. Potential of municipal woody biomass waste ash in the production of cold-bonded lightweight aggregates. *Journal of Building Engineering*. 2023;63(January):1-27. <https://doi.org/10.1016/j.jobe.2022.105392>
- [26] ASTM C618. Coal Fly Ash and Raw or Calcined Natural Pozzolan for Use. *Annual Book of ASTM Standards*. 2019;04.02:1-5. <https://doi.org/10.1520/C0618-19>
- [27] ASTM C127. Relative Density (Specific Gravity) and Absorption of Coarse Aggregate. *Annual Book of ASTM Standards*. 2015;04.02:1-5. <https://doi.org/10.1520/C0127-15>
- [28] British Standards Institution BSI. Depth of penetration of water under pressure. BS EN 12390-8:2000. 2003;(August):420-57. ICS 91.100.30 , Feb., 2009 .
- [29] ASTM C1202. Electrical Indication of Concrete's Ability to Resist Chloride Ion Penetration. *Annual Book of ASTM Standards* [Internet]. 2013;04.02:1-8. <https://doi.org/10.1520/C1202-19>
- [30] ASTM C157. Length Change of Hardened Hydraulic-Cement Mortar and Concrete. *Annual Book of ASTM Standards*. 2014;04.02:1-7. https://doi.org/10.1520/C0157_C0157M-08
- [31] Liu X, Chia KS, Zhang MH. Water absorption, permeability, and resistance to chloride-ion penetration of lightweight aggregate concrete. *Construction and Building Materials* [Internet]. 2011;25(1):335-43.. <https://doi.org/10.1016/j.conbuildmat.2010.06.020>
- [32] Güneyisi E, Gesoğlu M, Booya E, Mermerdaş K. Strength and permeability properties of self-compacting concrete with cold bonded fly ash lightweight aggregate. *Construction and Building Materials*. 2015;74:17-24. <https://doi.org/10.1016/j.conbuildmat.2014.10.032>
- [33] Du H. Properties of ultra-lightweight cement composites with nano-silica. *Construction and Building Materials* [Internet]. 2019;199:696-704. <https://doi.org/10.1016/j.conbuildmat.2018.11.225>
- [34] Güneyisi E, Gesoglu M, Azez OA, Öz HÖ. Physico-mechanical properties of self-compacting concrete containing treated cold-bonded fly ash lightweight aggregates and SiO₂ nano-particles. *Construction and Building Materials*. 2015;101:1142-53. <https://doi.org/10.1016/j.conbuildmat.2015.10.117>
- [35] Ahmad S, Adekunle SK, Maslehuddin M, Azad AK. Properties of Self-Consolidating Concrete Made Utilizing Alternative Mineral Fillers. *Construction and Building Materials*. 2014;68:268-76. <https://doi.org/10.1016/j.conbuildmat.2014.06.096>
- [36] Oh BH, Cha SW, Jang BS, Jang SY. Development of high-performance concrete having high resistance to chloride penetration. *Nuclear Engineering and Design*. 2002;212(1-3):221-31. [https://doi.org/10.1016/S0029-5493\(01\)00484-8](https://doi.org/10.1016/S0029-5493(01)00484-8)
- [37] Du H, Du S, Liu X. Effect of nano-silica on the mechanical and transport properties of lightweight concrete. *Construction and Building Materials* [Internet]. 2015;82:114-22. <https://doi.org/10.1016/j.conbuildmat.2015.02.026>

- [38] Zhang MH, Li L, Paramasivam P. Shrinkage of high-strength lightweight aggregate concrete exposed to dry environment. *ACI Materials Journal*. 2005;102(2):86-92. <https://doi.org/10.14359/14301>
- [39] Zhuang YZ, Zheng DD, Ng Z, Ji T, Chen XF. Effect of lightweight aggregate type on early-age autogenous shrinkage of concrete. *Construction and Building Materials* [Internet]. 2016;120:373-81. <https://doi.org/10.1016/j.conbuildmat.2016.05.105>
- [40] Sadrumontazi A, Barzegar A. Assessment of the effect of nano-SiO₂ on physical and mechanical properties of self-compacting concrete containing rice husk ash. 2nd International Conference on Sustainable Construction Materials and Technologies. 2010; Universita Politecnica delle Marche, Ancona, Italy. ISBN 978-1-4507-1488-4. www.claisse.info/Proceedings.htm, 2010.
- [41] Wang, X. F., Huang, Y. J., Wu, G. Y., Fang, C., Li, D. W., Han, N. X., and Xing F. Effect of nano-SiO₂ on strength, shrinkage and cracking sensitivity of lightweight aggregate concrete. *Construction and Building Materials*. 2018;175:115-25. <https://doi.org/10.1016/j.conbuildmat.2018.04.113>
- [42] Gesoglu M, Özturan T, Güneyisi E. Shrinkage cracking of lightweight concrete made with cold-bonded fly ash aggregates. *Cement and Concrete Research*. 2004;34(7):1121-30. <https://doi.org/10.1016/j.cemconres.2003.11.024>
- [43] Wiegink K, Marikunte S, Shah SP. Shrinkage cracking of high-strength concrete. *ACI Materials Journal*. 1996;93(5):409-15. <https://doi.org/10.14359/9844>